13th International Symposium on Turbulence and Shear Flow Phenomena (TSFP13)
Montreal, Canada, June 25–28, 2024

EXPERIMENTAL AND NUMERICAL INVESTIGATION OF SUPERSONIC MULTI-STREAM RECTANGULAR JET FLOW USING STEADY BLOWING CONTROL

Matthew A. Qualters, Melissa Yeung, Seth W. Kelly, Yiyang Sun, Fernando Zigunov, Mark N. Glauser
Department of Mechanical and Aerospace Engineering
Syracuse University, Syracuse, NY 13244, USA
maqualte@syr.edu, meyeung@syr.edu, skell101@syr.edu, ysun58@syr.edu, fzigunov@syr.edu, mglauser@syr.edu

Datta V. Gaitonde, Thakare Pranav
Department of Mechanical and Aerospace Engineering
The Ohio State University, Columbus, OH 43210, USA
gaitonde.3@osu.edu, thakare.5@osu.edu

ABSTRACT

Active control is applied through experimentation and computation to a complex supersonic multi-stream rectangular jet nozzle configuration in an attempt to mitigate the unsteadiness of the resultant flow field and therefore prompt the reduction of unwanted acoustic tones. Mach = 1.6 and Mach = 1.0 flows are separated by a splitter plate within the jet nozzle until slightly upstream of the nozzle exit where these flows are allowed to mix, resulting in a complex shock structure and multiple shear layers. An array of sonic, steady micro-jets is placed slightly downstream of the splitter plate tip in order to interact with the shear layer being formed there. Far-field pressure measurements and time-resolved schlieren imaging of the experimental flow are recorded to analyze and correlate with robust two-dimensional and three-dimensional numerical simulations of the flow. By utilizing both experimental and numerical data, the efficacy of the control system and the qualitative implications to the surrounding flow field can be discerned.

BACKGROUND

This study investigates a three-stream engine design consisting of a main stream, a fan stream, and a third stream. The main and fan streams are assumed to be fully mixed before entering the nozzle, and is referred to as the core stream. The addition of the cooled third stream has been found to aid in thermal management and reduce supersonic signature (Papamoschou & Debiasi (2001); Berry *et al.* (2016); Bruening & Chang (1999)). The nozzle geometry features a single-sided expansion ramp (SERN), a splitter plate that separates the two canonical flows, and an aft-deck to represent the aircraft anatomy. The Multi-Aperture Rectangular SERN (MARS) at the Syracuse University Skytop Turbulence Labs (figure 1) is used in conjunction with 3D Large Eddy Simulations and 2D Direct Numerical Simulations (figure 2) to understand the intricate flow physics within the nozzle and the emergent plume. At operating conditions, the core and third streams utilize nozzle pressure ratios (NPR) of 4.25 (M = 1.6) and 1.89 (M = 1.0), respectively. At the splitter plate trailing edge (SPTE), the mixing of the two streams generates a vortex shedding that convects downstream along the aft-deck, forming the splitter plate shear layer (SPSL). The turning associated with the thick SPTE initiates a relatively strong primary shock and a subsequent shock train, which interacts with different boundary layers and the shed vortices. Most notably, a 34 kHz tone ($St = 3.3$) originating from the shedding instability at the SPTE dominates the flow field and far-field acoustics (Berry (2016)).

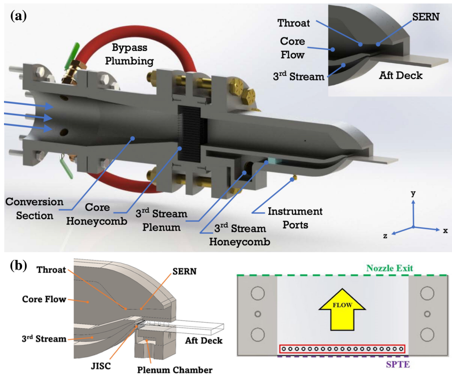

Figure 1. (a) MARS rig used at Skytop Turbulence Labs (Berry *et al.* (2017)) (b) Experimental micro-jet array with top down view of aft-deck plate.

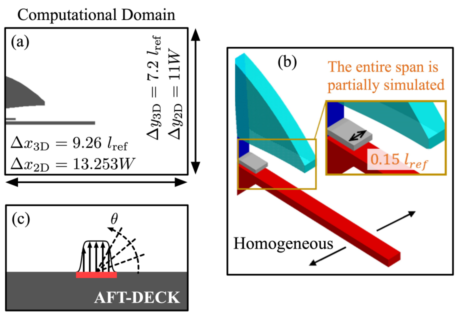

Figure 2. (a-b) 3D LES and 2D DNS computational domains with (c) 2D DNS actuation control schematic.

CONTROL STRATEGY

Extensive experimental and computational work has been carried out to investigate various control strategies with the goal of mitigating the resonant tone. Modifications have been made in the splitter plate proximity region, as this location was found to be most receptive to external disturbances. Previously, Gist (2022) introduced a spanwise wavenumber β to the SPTE, and found the stream-wise vorticity induced by the wavy splitter plate broke down the coherent structures associated with the signature high-frequency tone. This was consequently reflected in the far-field acoustic spectra through the elimination of the dominant frequency. The success of this passive control technique motivated the investigation into active flow control strategies, as active control holds the potential to be continuously adjusted to adapt to various flight conditions, making it a more practical alternative.

Jets in cross flow have been widely used to control various supersonic situations; Ali & Alvi (2015) provides a comprehensive background on jets in supersonic cross flow (JISC). Building upon this work and utilizing its findings to guide an active control arrangement, a steady-blowing micro-jet array was chosen for control. A nineteen-hole array of $2mm$ diameter holes, evenly spaced $4.11mm$ apart center-line to center-line is incorporated into the aft-deck plate a short distance downstream of the SPTE. The spanwise wavenumber corresponding to this configuration, $\beta = 0.8$, is the same as that of Gist (2022). Two parametric studies are conducted using this configuration, in which the JISC spatial location and the angle of the actuator blowing into the flow are varied.

EXPERIMENTAL TECHNIQUES

Two primary methods of experimental measurements were explored: pressure measurements, and time-resolved schlieren imaging. A series of nine G.R.A.S. microphones are placed in a 90-degree arc $85D_h$ downstream in the plane with the nozzle, where D_h is the hydraulic diameter, sampling at 100 kHz allowing time-resolved information to be captured. The shedding instability emanating from the SPTE dominates the 120-degree microphone signal, highlighted red in figure 3. This microphone location will be discussed at length in the results section.

A Photron SA-Z high-speed camera recording at 100 kHz captures time-resolved data via a z-type schlieren system as described by Settles (2001), with a vertically orientated knife edge. Illuminated by a Luminus CBT-120 green LED light source, the system also utilizes two 12.5-inch diameter parabolic mirrors with a focal length of 100.5 inches. The micro-jet array is introduced by drilling the nineteen $2mm$ holes into the poly-carbonate aft-deck plate. An aluminum plenum chamber, fed by a 100 psig Kaiser compressor, is bolted onto the underside of the aft-deck, as shown in figure 1b, and forces air through the JISC array. The experimental Reynolds number of $Re_{D_h} = 2.74 \times 10^6$ is derived using experimental information and the isentropic relations. It should be noted that the schlieren and far-field acoustic results were obtained simultaneously – the presence of the parabolic mirrors in the anechoic chamber diminished its efficacy slightly as they cannot be acoustically treated. However little deviation was found between results with and without the presence of the schlieren setup, thus acoustics taken simultaneously with their schlieren counterparts were chosen for this study.

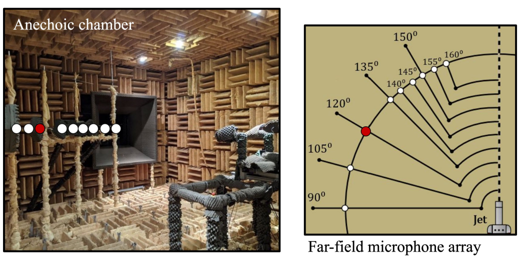

Figure 3. Experimental anechoic chamber and far-field microphone array.

NUMERICAL MODEL

Complementary 2D Direct Numerical Simulations (DNS) and 3D Large Eddy Simulations (LES) with spanwise periodic conditions have been performed (figure 2b). Figure 4 presents instantaneous views from each. Detailed analyses (not shown) indicate that the dominant flow physics within the nozzle is largely two-dimensional, except in the region close to the sidewalls, with the 2D simulations capturing the same overall flow physics within the nozzle. As a parametric study is to be performed, the 2D model is used for the remainder of this study to limit computational costs.

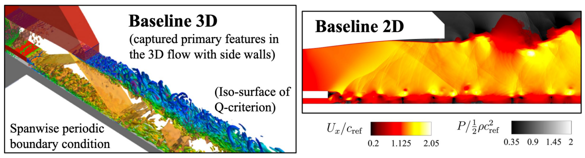

Figure 4. Flow fields obtained from 3D LES and 2D DNS.

The 2D simulations were performed using *CharLES* (Brès & Lele (2019); Brès *et al.* (2018)), which solves the compressible Navier-Stokes equations using a second-order finite-volume method and a third-order Runge-Kutta temporal scheme. A relative-solution-ENO scheme is utilized to capture shock structures. The sonic micro-jet actuator is introduced using a hyperbolic tangent velocity profile (figure 2c) with a slot length equivalent to the experimental length scale of $2mm$.

SPOD

Spectral Proper Orthogonal Decomposition (SPOD) techniques are applied to the time-resolved schlieren data sets to break down the complex turbulent dynamics of the system and isolate certain flow features that may be used to quantify the efficacy of the different control arrangements tested. SPOD as a means to extract coherent structures traces back to Lumley (1967), applications of the technique similar to those presented here were piloted by Glauser *et al.* (1987), and more recently placed in the context of newer methods by Schmidt & Colonius (2020).

SPOD was applied to the schlieren data sets by applying a Fourier transform and block averaging with 1,024 images per block with a 50 % overlap between the 96 blocks. A Hamming window is individually applied to every pixel location within the time series. An orthogonal decomposition is computed via a Singular Value Decomposition (SVD) on the cross-correlation matrix of the transformed data. This eigenvalue decomposition yields a basis for the distribution of energy (quantified as $(d\rho/dx)^2$) across all frequencies, facilitating identification of prominent frequencies in the flow, and the spatial form of the features at those frequencies.

RESULTS

This section discusses the experimental and numerical results for the baseline and controlled flows. Active control is introduced along the aft-deck plate at various locations and angles. The locations are chosen based upon the surface pressure distribution, while the actuation angle (θ in figure 2c) is measured counter-clockwise from the stream-wise direction and tested within a range of $\theta \in [30°, 90°]$. Schlieren imaging is compared to simulated flow fields, and spectral analysis is performed to assess the control performance.

1. BASELINE FLOW

A comparison of the mean flow field obtained from simulation and the mean schlieren from the experiment is presented in figure 5. Two-dimensional shock structures leaving the nozzle exit are indicated with arrows, with the blue arrow being the nozzle lip shock, and the red being a reflected shock (R1). From simulation results, it is evident that the reflected shock is induced by a primary S1 shock that initiates near the splitter plate trailing edge (SPTE) region. When the S1 shock impinges on the nozzle wall, a shock-boundary-layer interaction (SBLI) occurs, resulting in flow separation and the R1 shock. The reflected R1 shock and the nozzle lip shock intersect downstream of the nozzle exit, where the location at which impingement along the aft-deck occurs is denoted as the drill region. Further downstream, the shock train interacts with the nozzle lip shear layer, denoted as the hub region. It is observed that actuation through the aft-deck plate displays some control authority over the drill and hub regions, as will be discussed later.

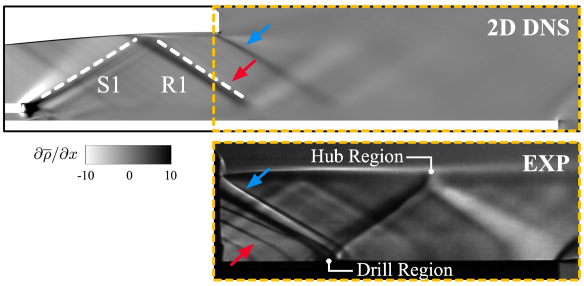

Figure 5. Comparison between simulation and experimental flow fields for the baseline case.

The SPOD is applied to the the baseline case using experimental schlieren images and the density flows field obtained from simulation to extract coherent structures from the turbulent flow, as shown in figure 6. In the eigen-spectra obtained from both experimental and numerical data, peaks are observed at the dominant frequency of $St = 3.3$ and its harmonics. The corresponding leading mode $\Phi_{i=1}$ at this frequency reveals the origin of this tone in the vortex-shedding mechanism due to the mixing between the core flow and third stream, suggesting the baseline flow features are dominated by this instability.

2. CONTROL: DOWNSTREAM STUDY

Since the region near the splitter plate trailing edge was found to be most receptive to external disturbances, control efforts have been directed toward modifications in this area. Due to experimental limitations, the micro-jet actuators are introduced through the aft-deck plate as close to the SPTE as possible, rather than through the splitter plate itself. Six different downstream locations for the JISC were then chosen based on the surface pressure on the deck plate gathered from LES simulation, as shown in figure 7, where plates A through F gradually actuate further downstream from the SPTE. Here, to examine the effects of the actuation location, the micro-jet is introduced perpendicular ($\theta = 90°$ in figure 2c) to the aft-deck at sonic speed.

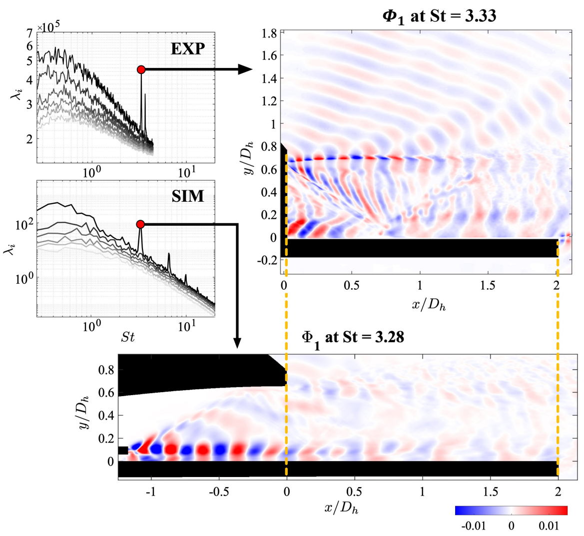

Figure 6. Baseline SPOD eigen-spectra for experiment and simulation with leading mode $\Phi_{i=1}$ shown at the resonant frequency.

Plate Name	Dist. from SPTE (mm)
A	4.13
B	5.56
C	11.1
D	16.69
E	20.02
F	26.7

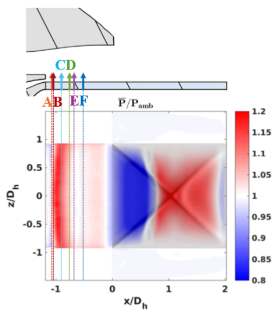

Figure 7. Experimental downstream actuation locations (Kelly (2024)) with baseline time-averaged surface pressure normalized by ambient pressure (Stack (2019)).

Far field acoustics results (figure 8) indicate that each case has little effect on the overall sound pressure level (SPL), with each closely tracking the nominal case at all angles except for the high frequency peak (HFP) found at the 120° microphone (see figure 3 for microphone locations). Focusing on the high frequency peak, some interesting trends can be observed, as displayed in figure 8. The acoustics of these tests display three separate trends. Plates A, B, and C, actuating into the high pressure region on the surface of the deck plate, split the peak into two: a lower frequency and a higher frequency peak both with the same magnitude as the original. The lower frequency of the pair has a wider peak and contains more energy while the high frequency of the pair has a narrower range but higher amplitude. Plates D and E, actuating into the low pressure region on the surface of the deck plate, create more of a sound pressure hump. A three-peaked structure is evident in the erstwhile singular peak region; the middle peak of the three is at approximately the same frequency as the nominal peak and contains the lowest energy. The other two humps, higher and lower in frequency, contain the major portion of the energy. Plate F, actuating the farthest downstream into the middle pressure region on the surface of the plate, returns the high frequency peak structure to a single peak, albeit wider and with a secondary minor hump embedded within the main structure; its frequency is slightly lower than that of the nominal high frequency peak structure. A general trend that can be observed is that the closer the JISC actuators are to the SPTE, the more shifted the HFP is in frequency and amplitude.

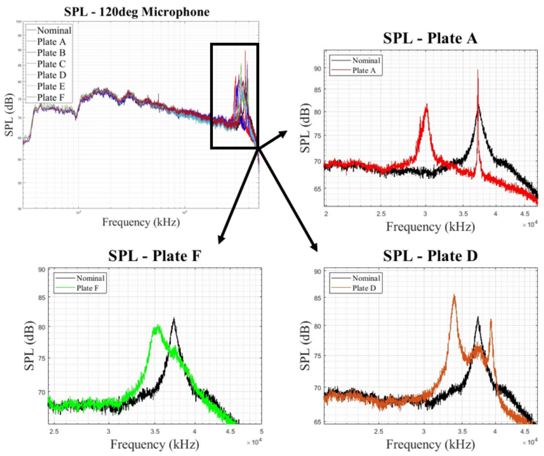

Figure 8. (a) 120° microphone SPL Spectra (b) HFP Plate A (c) HFP Plate F (d) HFP Plate D.

The schlieren images indicate that any actuation that introduces a new shock to the system will have significant influence over the drill region. Figure 9 compares the 2D simulation and experimental (Kelly (2024)) flow fields for representative control cases, with the dashed blue line representing the drill location in the baseline flow (see figure 5). In the control case with Plate A, the drill is pushed slightly upstream by a distance of $0.05D_h$, and this trend continues until it reaches a maximum at $0.225D_h$ upstream from the nominal location in the control case with Plate D. The simulations indicate that a new actuation-induced shock (A1) causes the reflected shock (R2) to impinge on the aft-deck further upstream compared to the baseline case, thus pushing the drill region further within the nozzle. The drill region continues to move upstream as the actuator is moved downstream until Plate D. After this point, the trend reverses i.e, further downstream actuation results in a gradual upstream location of the drill, but the movement is minimal. Simultaneously, the impingement location of the lip shock moves further downstream along the aft-deck, as indicated in the Plate F case, where the actuation is introduced furthest from the SPTE. This suggests that actuating in the high pressure region near the SPTE (Plates A–D, see figure 7 for pressure distribution) has influence over the drill, and actuating downstream in the lower pressure region (Plates D–F) affects the lip shock.

By taking the root mean square of the schlieren images, an example of which can be seen in figure 10, it is also shown that as the actuators progress downstream, the density fluctuations at the drill and hub increase, most notably in Plate F. The high-frequency peak information gathered from the SPOD processing on the schlieren images is consistent with the far field acoustics. It was also found that each case in this series increases the low-frequency shock unsteadiness which occurs around $St = 0.23$ in the baseline case.

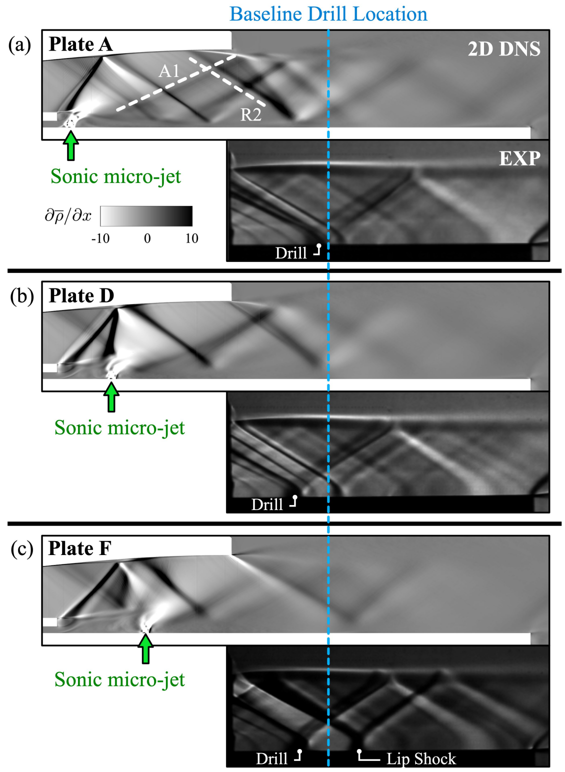

Figure 9. Comparison between simulation and experimental (Kelly (2024)) flow fields for (a) Plate A, (b) Plate D, and (c) Plate F control cases. The location of the drill region in the baseline flow is indicated as a dashed blue line for reference.

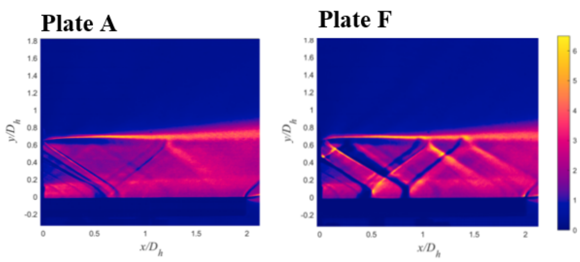

Figure 10. Root Mean Square – Schlieren

3. CONTROL: ANGLE STUDY

The angle of actuation is then varied in the lower pressure region at the same downstream location as Plate F, where figure 11 shows the configuration of all angled actuator cases. Four angles of $\theta = 90°$ (F), 60° (G), 45° (H), and 30° (I) were tested, with figure 12 showing their respective acoustic spectra at the 120° microphone (figure 3). Acoustically, little benefit is obtained from altering the angle at this downstream location. Plates G and I (60° and 30°, respectively) are interestingly identical to each other. However, they both increase the amplitude of the high frequency peak by around 6 dB with the slightest decrease in frequency compared to the nominal case. Plate H (45°) increases both the frequency and amplitude of the high frequency peak, while introducing another narrow yet large dB spike to the system. The other frequencies of the angled cases do not deviate notably when compared to the nominal. Plate F as discussed, 90°, is the most beneficial in terms of acoustic mitigation.

The schlieren measurements of the angled cases, as shown in figure 13, show similar characteristics as the acoustic data in

Plate Name	Angle (Relative to Core Flow)
F	90°
G	60°
H	45°
I	30°

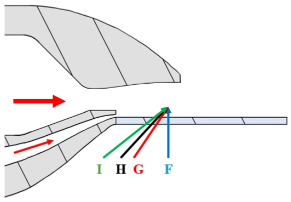

Figure 11. Angled actuator locations.

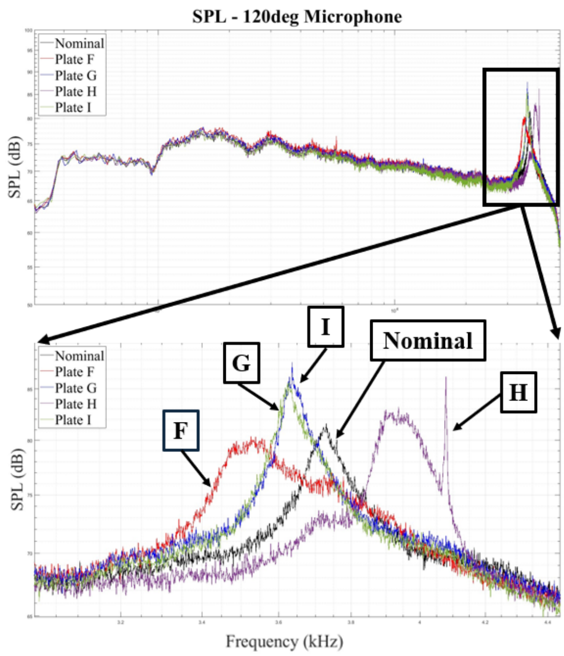

Figure 12. 120° microphone SPL Plot – Angled JISC Cases

that there is little change to the flow characteristics besides the minor shifting of the shape, frequency, and amplitude of the HFP compared to the 90° case. Compared to the baseline case, the results are as expected given the discussion of the downstream series. Actuation at this location at all angles is found to separate the drill and the lip shock impingement along the aft-deck, such that the drill moves upstream from the baseline location while the lip shock moves downstream. Variation in the actuation angle has minimal effect on the aforementioned shock structures. Higher regions of density fluctuation are also found after the drill and hub regions.

CONCLUSION

A complex supersonic multi-stream nozzle flow is investigated, which contains a Mach 1.6 core flow and a Mach 1.0 tertiary stream mixing downstream of a splitter plate separating the two flows. An upper nozzle surface and a lower deck plate form the upper and lower bounds of the configuration. The dominant frequency present throughout the flow-field and in far-field acoustics is confirmed to originate from the shedding instability generated from the mixing of the two canonical flows. Spectral proper orthogonal decomposition applied to the baseline schlieren and simulation datasets reveal the dominance of the high energy shedding instability. In an attempt to suppress the resonant tone, active flow control in the form of

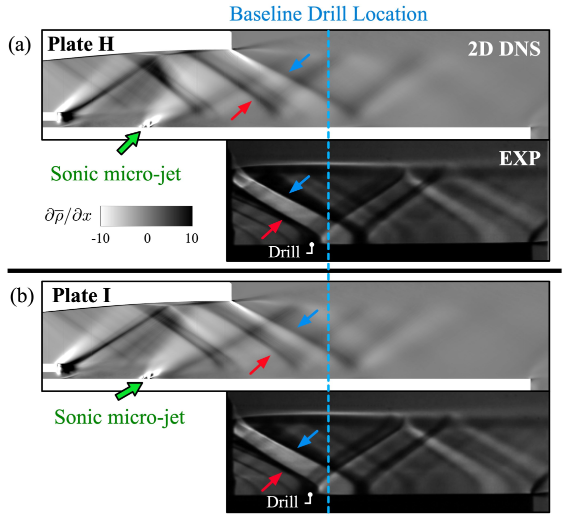

Figure 13. Comparison between simulation and experimental (Kelly (2024)) flow fields for (a) Plate H and (b) Plate I control cases. The location of the drill region in the baseline flow is indicated as a dashed blue line for reference.

steady-blowing micro-jet actuation on the aft-deck plate near the splitter plate trailing edge is implemented in experiments and simulations. A parametric study is conducted at various spatial locations and actuation angles, where the spatial locations are chosen based upon the pressure distribution along the aft-deck plate.

The drill location, where the nozzle lip and reflected shocks impinge on the aft-deck plate, is influenced by control introduced in the high pressure region. Far-field acoustics also show that the high frequency peak is split into two separate peaks. Actuating in the lower pressure region has minimal influence in the drill, but rather affects the shock emanating from the nozzle lip. Varying the actuation angle in this low pressure region has minimal influence on the shock structures and overall flow field, as all control cases at this location exhibit similar flow physics. A broadband frequency hump is also observed in the far-field acoustic spectra. This suggests that in order to achieve control authority over shock structures near the drill region, actuation should be introduced in the high pressure region near the splitter plate trailing edge. Conversely, actuation should be introduced in the low pressure region to influence the nozzle lip shock.

ACKNOWLEDGEMENT

This work was supported by the Air Force Office of Scientific Research (AFOSR) under award FA9550-23-1-0019 monitored by Dr. Gregg Abate (Program Officer). Simulations were performed at U.S. DOD HPCMPs and computing centers at Syracuse and Ohio State Universities.

REFERENCES

Ali, Mohd Yousuf & Alvi, Farrukh 2015 Jet arrays in supersonic crossflow—an experimental study. *Physics of fluids* **27** (12), 126102.

Berry, Matthew G 2016 Investigating the interaction of a supersonic single expansion ramp nozzle and sonic wall jet. PhD thesis, Syracuse University.

Berry, Matthew G, Magstadt, Andrew S, Glauser, Mark N, Ruscher, Christopher J, Gogineni, Sivaram P & Kiel, Barry V 2016 An acoustic investigation of a supersonic, multi-stream jet with aft deck: Characterization and acoustically-optimal operating conditions. In *54th AIAA Aerospace Sciences Meeting*, p. 1883.

Berry, Matthew G, Stack, Cory M, Magstadt, Andrew S, Ali, Mohd Y, Gaitonde, Datta V & Glauser, Mark N 2017 Low-dimensional and data fusion techniques applied to a supersonic multistream single expansion ramp nozzle. *Physical Review Fluids* **2** (10), 100504.

Brès, Guillaume A, Jordan, Peter, Jaunet, Vincent, Le Rallic, Maxime, Cavalieri, André VG, Towne, Aaron, Lele, Sanjiva K, Colonius, Tim & Schmidt, Oliver T 2018 Importance of the nozzle-exit boundary-layer state in subsonic turbulent jets. *Journal of Fluid Mechanics* **851**, 83–124.

Brès, Guillaume A & Lele, Sanjiva K 2019 Modelling of jet noise: a perspective from large-eddy simulations. *Philosophical Transactions of the Royal Society A* **377** (2159), 20190081.

Bruening, Greg B & Chang, Won S 1999 Cooled cooling air systems for turbine thermal management. In *Turbo Expo: Power for Land, Sea, and Air*, , vol. 78606, p. V003T01A002. American Society of Mechanical Engineers.

Gist, Emma D 2022 Exploring passive flow control techniques applied to a supersonic multistream rectangular nozzle. PhD thesis, Syracuse University.

Glauser, Mark N., Leib, Stewart J. & George, William K. 1987 Coherent structures in the axisymmetric turbulent jet mixing layer. In *Turbulent Shear Flows 5*, pp. 134–145.

Kelly, Seth 2024 On the control of a supersonic multi-stream rectangular nozzle. PhD thesis, Syracuse University.

Lumley, J. L. 1967 The structure of inhomogeneous turbulent flows. *Atmospheric Turbulence and Radio Wave Propagation* pp. 166–178.

Papamoschou, Dimitri & Debiasi, Marco 2001 Directional suppression of noise from a high-speed jet. *AIAA journal* **39** (3), 380–387.

Schmidt, Oliver T. & Colonius, Tim 2020 Guide to spectral proper orthogonal decomposition. *AIAA Journal* **58** (3), 1023–1033.

Settles, G. S. 2001 *Schlieren and Shadowgraph Techniques*. Springer Berlin Heidelberg.

Stack, Cory M 2019 Turbulence mechanisms in a supersonic rectangular multi-stream jet with an aft-deck. PhD thesis, The Ohio State University.